JOURNAL OF CATALYSIS 145, 318–326 (1994)

Oxidative Dehydrogenation of Propane on γ-Al_2O_3 Supported Vanadium Oxides

J. G. Eon,* R. Olier,† and J. C. Volta‡

*Instituto de Quimica, Departamento de Quimica Inorganica and NUCAT/UFRJ, Bloco A-631, Ilha do Fundao, 21945-970 Rio de Janeiro, Brazil; †Laboratoire de Physicochimie des interfaces, CNRS, Ecole Centrale de Lyon, 36 Avenue Guy de Collongue, BP 163, Ecully Cédex, France; and ‡Institut de Recherches sur la Catalyse, CNRS, 2 Avenue A. Einstein, 69626 Villeurbanne Cédex, France

Received July 2, 1992; revised June 4, 1993

γ-Al_2O_3 supported vanadium oxides have been prepared following the continuous adsorption method. The superficial loading and the nature of the precursor species were monitored by varying the pH of the impregnation ammonium vanadate solution. The vanadium coordination was investigated by UV–visible, near infrared, Raman, ^{51}V NMR, and ESR spectroscopies, respectively after drying, calcination and catalytic oxidative dehydrogenation of propane in the 300–450°C temperature range. It is shown that mainly tetrahedral V^{5+} cover the alumina surface. Bridging V–O–V groups from the two-dimensional VO_4 array, occurring at high coverage, are suggested to be the active sites for catalytic oxidation. These species are converted to vanadyl ions ($V{=}O^{2+}$) in a $C4_v$ environment during propane oxidation. A mechanism for the structural transformation is proposed.

INTRODUCTION

Supported vanadium oxides have been studied for a long time as catalysts for hydrocarbon oxidation and have recently been the object of new structural and kinetic investigations (1–7). The coordination of vanadium and the superficial structure of the so-called monolayer have been extensively studied combining infrared (8), Raman (9, 10), and ^{51}V NMR (11) spectroscopies, as well as X-ray absorption fine structure (EXAFS), X-ray absorption near-edge structure (XANES) (12), and radial electron distribution of X-rays measurements (13). It appears that the superficial coverage and the chemical properties of the support are the important parameters defining the monolayer structure. The influence of the deposition method seems to be secondary when the catalysts have been calcined at high temperature (>500°C). Thus, a reasonably coherent characterization has been obtained for vanadium oxides deposited on alumina, silica, or titania by grafting or impregnation techniques (8–13, 15). However, an exact description of the active site and of the structural transformations occurring during the catalytic reaction is not yet available. So far, only mechanistic speculations involving single (or paired) oxohydroxy vanadium have been published (14). This situation is clearly not representative as polymeric vanadates are currently observed on many supports. In the case of TiO_2(-Anatase), it has been recently demonstrated by laser Raman spectroscopy (LRS) that the distribution of monomeric and polymeric vanadates changes depending on the vanadium coverage. The amount of monomeric vanadates is higher at low vanadia loadings, and then they react to form polymeric vanadates as the loading increases (10, 15).

In this work, we study the influence of the degree of condensation of vanadium, as determined by different physicochemical tools, on the catalytic properties of VO_x/γ-Al_2O_3 catalysts for the oxidative dehydrogenation of propane (ODH). Catalysts have been prepared by the continuous adsorption method. This technique was considered to be suitable for obtaining polymeric species at high coverage, as V–O–V linkages are present in vanadate polyanions for solutions in the 2–7 pH range (16). We propose a structural model for the catalytic site reduction from our spectroscopic and catalytic results.

EXPERIMENTAL

VO_x/γ-Al_2O_3 catalysts were prepared by percolating a 0.05 *M* ammonium vanadate solution through a non-porous (200 m^2g^{-1}) γ-alumina support bed until saturation was reached (15 ml of solution for 100 mg of the support). The pH of the solution was previously adjusted with nitric acid. Three samples were prepared at pH 7.0, 4.5, and 2.5 for which different vanadate polyanions can be prepared in solution (*meta*vanadates $V_3O_9^{3-}$ and $V_4O_{12}^{4-}$ with tetrahedrally coordinated vanadium and decavanadates $V_{10}O_{28}^{6-}$ and $V_{10}O_{28}H^{5-}$ with octahedrally coordinated vanadium respectively) (16). They were further washed with acetone and then calcined under air flow at atmospheric pressure according the following procedure: temperature was raised linearly for 2 h up to 120°C, kept

0021-9517/94 $5.00

constant at 120°C for 4 h for drying, raised linearly up to 500°C, and then maintained for 16 h at 500°C.

The vanadium content was determined by atomic absorption spectroscopy. The different samples are designated in the text by combining the letters D (dried with acetone at room temperature), C (calcined at 500°C), or T (tested for propane ODH) and a number corresponding to the entire value for pH of the adsorption solution.

The three catalysts were tested for oxidative dehydrogenation of propane in a flow system. The solid (100 mg) was deposited on a fixed bed in a quartz microreactor (U-tube, 13 mm diameter) operating under atmospheric pressure. The catalytic zone was isothermal (6 mm height, 0.8 cm^3 volume) with a postcatalytic zone (0.4 cm^3). Analysis of the reactants and reaction products was done by on-line chromatography (7). For the permanent gases and H_2O, a Delsi IGC 120 MB gas chromatograph equipped with a thermal conductivity detector was used. Two columns were operated in parallel, a 3 m × $\frac{1}{4}$ in. molecular sieve column to separate O_2 and CO and a 2 m × $\frac{1}{4}$ in. Porapak Q to separate CO_2 and H_2O. Hydrogen was the carrier gas. For the organic products, a Delsi IGC 120 FB gas chromatograph equipped with a flame ionization detector was used. The carrier gas was nitrogen. Three columns were operated in parallel: a 4 m × $\frac{1}{8}$ in. Durapak column to separate light hydrocarbons (methane, ethane, ethene, propane, propene), a 3 m × $\frac{1}{8}$ in. Carbowax column to separate oxygenates (ethanal, propanal, acetone, acrylaldehyde), and a 2 m × $\frac{1}{8}$ in. AT column to separate acids (acetic, propionic, and acrylic acids). The last column was situated in a hot box together with the four injection valves which were monitored by a Spectra Physics computer. The reactor was directly connected to the hot box to prevent any condensation of the reaction products. Catalytic runs were automatically monitored by the computer. The gas mixture containing propane (2 vol%), O_2 (19.6 vol%) and N_2 (78.4 vol%) was fed at a flow rate of 50 ml/min. and the temperature was varied from 300 to 450°C during a 16-h period. Two analyses were performed at each temperature. No deactivation was observed.

The three catalysts were characterized, respectively, after vanadate adsorption and drying (D), after calcination (C), and after the catalytic test (T) by different physicochemical techniques. UV–visible and near IR spectra (diffuse reflectance) were recorded on a Perkin–Elmer Lambda 9 spectrometer equipped with an integration sphere. ^{51}V NMR spectra were obtained on a Bruker MSL-300 spectrometer operating at 78.86 MHz under static conditions. The number of scans was 10,000 for vanadium. The spectra are referenced to $VOCl_3$. ESR spectra were recorded with a Varian E9 spectrometer using the 9.3 GHz (X band) microwave frequencies. In X-band mode, a dual cavity was used and the g values were measured by comparison with a DPPH (Diphenylpicrylhydrazyl) sample (g = 2.0036). In Q-band mode, they were determined by measuring the magnetic field, H, and the microwave frequency. Raman spectra were obtained on a Dilor Omars 89 spectrophotometer equipped with an intensified photodiode array detector. The emission line at 514.5 nm from an Ar^+ ion laser (Spectra Physics, Model 164) was used for excitation. The power of the incident beam on the sample was 36 mW. Time of acquisition was adjusted according to the intensity of the Raman scattering; 500 spectra were accumulated in order to improve signal to noise ratio (exposure time: 10 s/scan). The wavenumber values obtained from the spectra were accurate to within about 2 cm^{-1}. In order to reduce both thermal and photodegradation of samples, the laser beam was scanned on the sample surface by means of a rotating lens. The scattered light was collected in the back-scattering geometry.

RESULTS

(a) *Vanadium Loading*

The vanadium weight content of the three catalysts and the resultant coverages are given in Table 1. The coverage Θ was calculated from the V_2O_5 unit cell area $A(VO_{2.5})$ = 0.165 nm^2 in the (100) V_2O_5 plane) and from the initial BET area of the support. It was observed that the specific area was practically unaffected by the deposition process.

As expected for a basic support, we note that the superficial loading increases as the pH of the adsorption solution turns more acidic and goes farther from the zero point of charge of γ-Al_2O_3 (8.1 as measured by mass titration (17)). Thus, approximately one-third of an equivalent monolayer is obtained at pH 7 and two-thirds at pH 2.5.

(b) *Catalytic Study*

Results for propane ODH are given in Table 2. With the exception of sample C7, carbon balance is satisfactory. No oxygenates could be detected in any case. Prep-

TABLE 1

Vanadium Weight Content and Superficial Coverage as a Function of the pH of Vanadate Adsorption Solution (Unit Area $A(VO_{2.5})$ = 0.165 nm^2)

Sample	v (% mass)	Coverage
D2	6.8	0.65
D4	5.6	0.54
D7	2.9	0.28

TABLE 2

Catalytic Results for Propane Oxidative Dehydrogenation on VO_x/γ-Al_2O_3

Catalysts	Temperature (°C)	Conversion (%)		Selectivity (%)				
		C_3H_8	O_2	C_3H_6	C_2H_4	CO_2	CO	Σ
C2	300	1.0	0.7	—	—	—	—	—
	350	13.5	6.1	41	0.4	17.5	28	86
	375	22.3	10.5	27.6	—	24	39	90
	400	40.1	19.9	15	1	25	45	85
C4	300	1	0.2	—	—	—	—	—
	350	8.8	2.9	50.4	—	14	16	80
	375	16.9	6.4	33.6	—	18	18	70
	400	26	10.9	28.2	—	22.4	26	77
C7	400	7.5	—	58.4	—	12.1	—	70
	450	23.7	—	35	—	18.2	—	78

arations at acidic pH (C2 and C4) are very efficient for propane activation since they work about 200°C below the temperature range usually reported for this reaction (500°C for the VMgO system (18)). In Fig. 1, propene selectivity is plotted as a function of the propane conversion for the three catalysts. It can be observed that all points fit the same curve and we can thus postulate that the same type of active site is present at the surface of the three catalysts, which should thus differ only by the superficial site concentration.

(c) *Diffuse Reflectance Spectroscopy*

Figure 2 shows the spectra of the solids in the UV–visible region after deposition and drying (D) and after catalytic test (T). A high-intensity charge transfer band in the 300–450 nm region and a large band in the 700–800 nm range are observed for all samples. The absorption band at 420–480 nm is characteristic of V^{5+} in octahedral environment, while it is considered that the band at 300 nm is due to V^{5+} in a tetrahedral environment (3). The *d–d* transitions of V^{4+} in a distorted octahedral symmetry give two broad bands at 770 and 625 nm (19).

Spectra recorded with precursors D7 and D2 (the curve for D4 is actually identical) present two bands located, respectively, at 320 and 450 nm, showing that deposited vanadates maintain the valence and the environment of the initial solution species, i.e., tetrahedral V^{5+} for sample prepared at pH 7.0 and preferentially octahedral V^{5+} for samples prepared at pH 4.0 and 2.5. Some traces of octahedral V^{4+} must however be present as very weak bands are observed at 700–800 nm.

After calcination, a shift is observed in the charge transfer band from 320 nm (D7) to 350 nm (C7) and from 450 nm (D2, D4) to, respectively, 420 and 380 nm (C2 and C4), indicating, as far as UV–visible allows this interpretation, an evolution of the vanadium superficial state to a mixture of tetrahedral and octahedral environments. These bands are practically not modified after the catalytic test. However, a significant fraction of vanadium is then reduced to V^{4+}, as it can be seen in Fig. 2 from the appearance of the band at 700–800 nm. Interestingly this reduced fraction is growing from T7 to T2 similarly with the increase of propane conversion. Figure 3 shows the near infrared spectra in the 1300–2500 nm region for the precursor D2 (as this exhibits the strongest effect) as compared with the pure γ-Al_2O_3 support. The support presents five absorption bands at 1385, 1450, 1882, 1930, and 2230 nm (7220, 6900, 5310, 5180, and 4480 cm^{-1}, respectively) which can be divided into three groups attributed to vibrational overtones and combination fre-

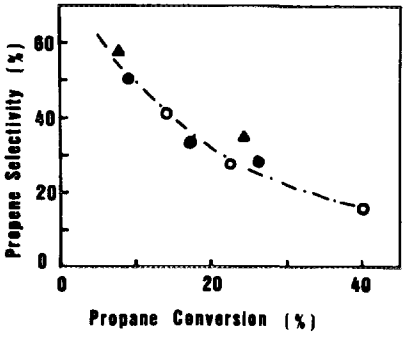

FIG. 1. Propene selectivity as a function of the propane conversion: (○) C2, (●) C4, and (▲) C7.

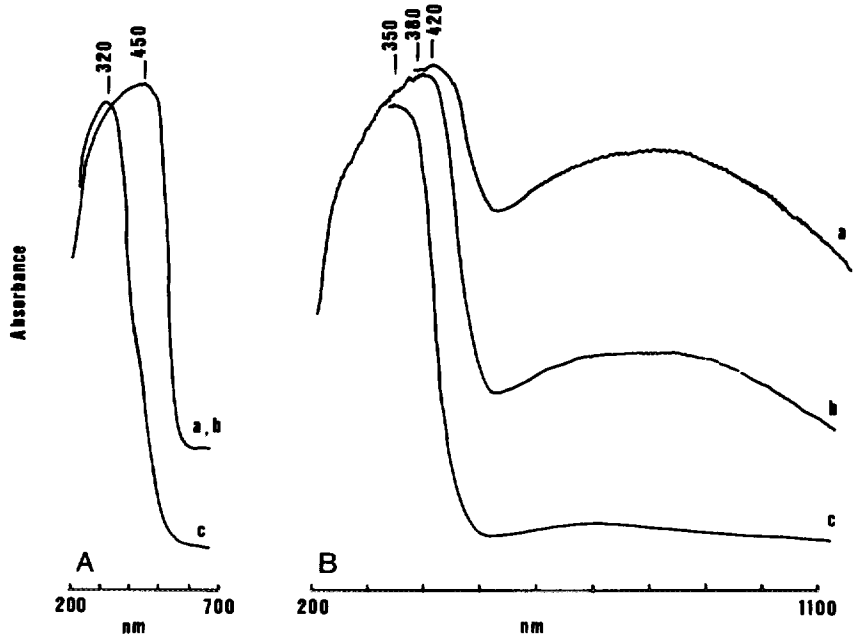

FIG. 2. UV–visible reflectance spectra at room temperature. (A) solids after deposition and drying: (a, b) solids D2 and D4 and (c) solid D7; (B) solids after propane oxydehydrogenation test: (a) solid T2, (b) solid T4, and (c) solid T7.

quencies of the OH superficial hydroxyls. Bands localized at about 7000, 5200, and 4400 cm^{-1} are respectively attributed to $2\nu(H_2O)$ or $2\nu(OH)$, $\nu + \delta$ (H_2O), and $\nu + \delta$ (OH) (19). The two intermediate bands at 5310 cm^{-1} (1882 nm) and 5180 cm^{-1} (1930 nm) show consequently the existence of two different types of adsorbed water molecules. Similar broad bands observed at 6850 and 5260 cm^{-1} for partially hydrated silica have been attributed to capillary-condensed water (20). By comparison, we suggest that the sharp bands observed in this work at 1385 nm (7220 cm^{-1}) and 1882 nm (5310 cm^{-1}) for hydrated γ-alumina might be attributed to H_2O molecules coordinated to Lewis acid sites and we assign the two broad bands at 1450 nm (6900 cm^{-1}) and 1930 nm (5180 cm^{-1}) to physisorbed water. Figure 3 shows that vanadate adsorption is accompanied by a strong decrease of the two sharp bands observed at 1385 and 1882 nm. Both bands disappear in the spectrum of D2. At the same time, the $\nu + \delta$ (OH) band at 2230 nm strongly decreases and a new band at 2260 nm emerges. This band is attributed to vanadium bonded hydroxyl groups. These results indicate that the surface H_2O and OH groups are displaced by surface vanadate species. This point is discussed later.

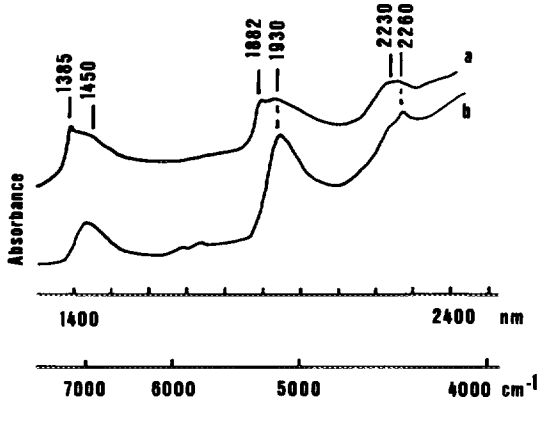

FIG. 3. Near infrared spectra of (a) γ-alumina support and (b) precursor D2 after vanadate adsorption.

(*d*) ^{51}V *NMR Spectroscopy*

Figures 4 and 5 show the wide line NMR spectra of ^{51}V vanadium obtained respectively after deposition and drying (D) and after calcination (C). Vanadium oxide surface layers on alumina and titania have been widely studied using solid state NMR spectroscopy (11). The two signals observed at about 310 and 540 ppm have been attributed respectively to octahedral (six-coordinated) and tetrahedral (four-coordinated) species. It has been possible to estimate the connectedness (number of bridging oxygens of the vanadate ion) in view of the anisotropy of the signal. Eckert and Wachs have shown a strong broadening and an enhancement of the chemical shift anisotropy of the signal when going from *ortho-* to *pyro-* and *meta*vanadates corresponding, respectively, to Q^0, Q^1, and Q^2 species (11) (see Table 4).

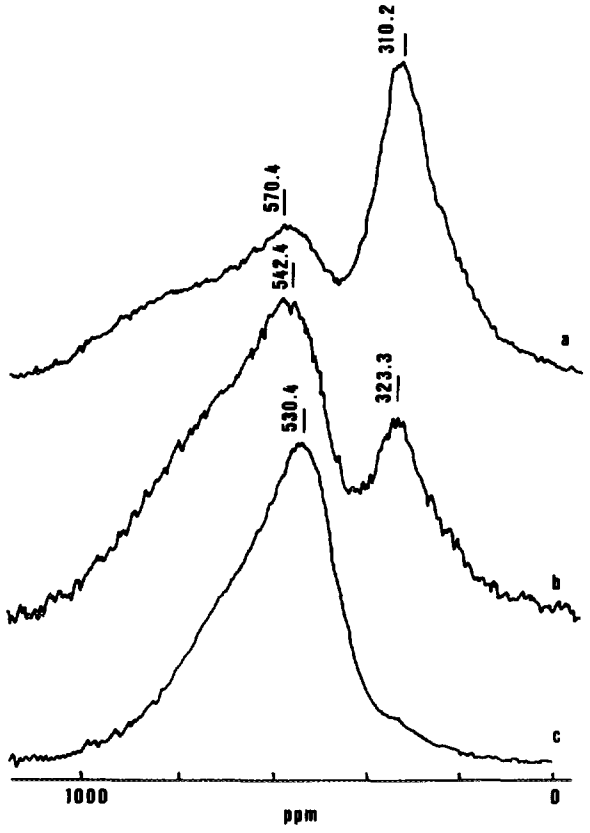

FIG. 4. ^{51}V NMR spectra after vanadate adsorption: (a) solid D2, (b) solid D4, and (c) solid D7.

Figure 4 shows that the local environment of the superficial vanadium species of the precursor is well defined by the initial vanadate solution: the chemical shift characterizes tetrahedral species for D7 (530.4 ppm), tetrahedral and octahedral species for D4 (542.4 and 323.3 ppm) and nearly all octahedral species for D2 (310.2 ppm). The same evolution has been noted by other authors as a function of the superficial coverage: diluted superficial vanadates have been interpreted as monomeric vanadyls; as coverage tends to one monolayer, octahedral polymeric species have been assumed to be preferentially formed (15). Note, however, that the primary variable in our case is not superficial concentration but vanadium environment as a function of the initial pH adsorption solution. After calcination, Fig. 5, the vanadium environment changes mostly towards tetrahedral species. Indeed some equilibrium between both coordinations seems to exist whatever the pH of adsorption, as all spectra present some octahedral component in addition to the predominant tetrahedral signal. According to Ref. (11), the strong anisotropy of the tetrahedral signal suggests that all tetrahedral species are highly connected, characterizing linear chains or bidimensional vanadate arrays.

TABLE 3

Spin Hamiltonian Parameters Measures on T2 Samples (after ODH) Compared with Amorphous V_2O_5 Parameters According to Ref. (18)

Spin parameters	VO_x/γ-Al_2O_3	Amorphous V_2O_5
$g_\parallel$	1.919	1.913
$g_\perp$	1.982	1.985
$A_\parallel$	190 Gauss	176 Gauss
$A_\perp$	70 Gauss	66 Gauss

No significant variation is noted for solids after the catalytic test. Figure 6 shows that, after oxidative dehydrogenation of propane, predominant species are tetrahedral vanadates (the lines are slightly shifted to approximately 580 and 320 ppm).

(e) ESR Spectroscopy

ESR spectra for calcined and dried samples were not recorded as it was clear by UV-visible spectroscopy that the V^{4+} amount was negligibly small. Figure 7 shows the ESR spectrum given by sample T2 after oxidative dehydrogenation of propane at 400°C. The spectrum recorded at room temperature is well resolved and can be attributed to an unpaired electron on a V^{4+} ion in an axially distorted symmetry (VO^{2+} in C4v environment) (21). The spin Hamiltonian parameters are listed in Table 3. They are rather close to the values observed with amorphous

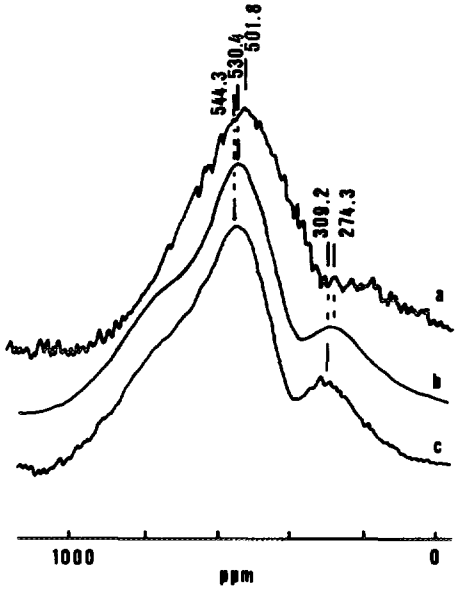

FIG. 5. ^{51}V NMR spectra after calcination at 500°C: (a) solid C2, (b) solid C4, and (c) solid C7.

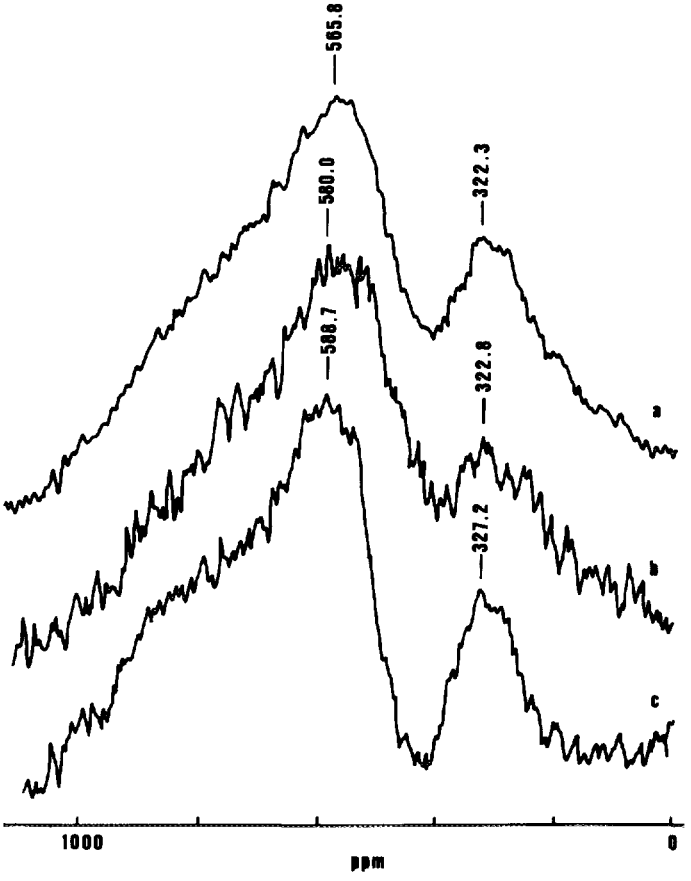

FIG. 6. ^{51}V NMR spectra after oxidative dehydrogenation of propane: (a) solid T2, (b) solid T4, and (c) solid T7.

V_2O_5 (22) and given in Table 3 for comparison. By quantitative determination using DPPH as a reference, we found that 4% of the vanadium had been reduced. The spectra acquired for the two other samples T4 and T7 were very similar to the spectrum of T2. They differed only with respect to the intensity of the lines, confirming the trend observed by UV–visible spectroscopy. The degree of reduction increases in the order T7 < T4 < T2.

(*f*) *Raman Spectroscopy*

Combining Raman and ^{51}V NMR spectroscopy provides essential information for analyzing vanadium oxide layer structures. However, we were able to record a signal only in the case of calcined C2, C4, and C7 samples. The other solids showed excessive fluorescence background. The spectra are presented in Fig. 8. We observe a set of common bands appearing with variable and weak intensity in the three cases at 820, 875, 900 and 945 cm^{-1}. These bands are assigned to the symmetric stretching of V=O in tetrahedral species: possible attributions may be deduced from literature data summarized in Table 4 (9). A large band is also present at 962 cm^{-1} in C7 spectrum and grows in intensity as it is shifting to 981 cm^{-1} for C4 and 994 cm^{-} for C2. Roozeboom *et al.* (23) have attributed this band to polymeric octahedral species by comparison with the spectrum of the decavanadate ion. However, this interpretation would conflict with the results of ^{51}V NMR reported here and with other recent studies (comparing at equal coverage) (10, 12), showing that vanadium has tetrahedral environment. According to more

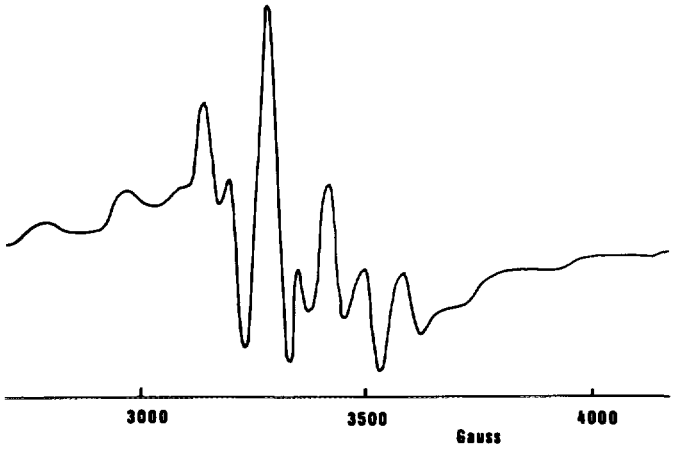

FIG. 7. ESR spectrum of VO_x/γ-Al_2O_3 prepared at pH 2.5 after oxidative dehydrogenation of propane.

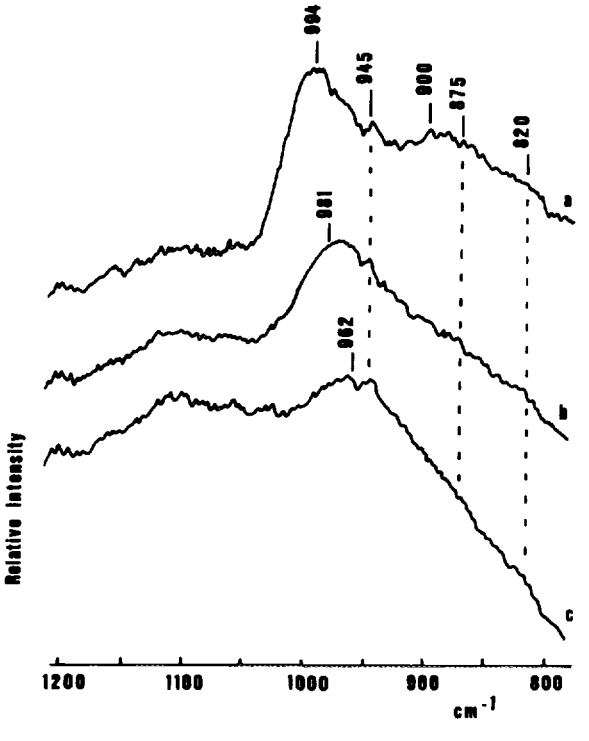

FIG. 8. Raman spectra of VO_x/γ-Al_2O_3 after calcination at 500°C: (a) solid C2, (b) solid C4, and (c) solid C7.

TABLE 4

V=O Vibration Frequencies as a Function of Vanadate Connectedness (9)

Vanadate species	ν (cm^{-1})	Connectedness
VO_4^{3-}	820–850	Q^0
$V_2O_7^{4-}$	873–912	Q^1
$(VO_3^-)_n$	927–955	Q^2
$V_{10}O_{28}^{6-}$	999	
V_2O_5	1025	

Note. The connectedness is defined as the number of other VO_n polyhedra to which the vanadate species is linked by sharing oxygen atoms (30). The symbol Q_s ($s = 0, 1, \ldots, 6$) is used to denote the corresponding vanadate.

recent works (9, 10), superficial vanadate species are hydrated under ambient conditions. Both hydrated polyvanadate chains and monomeric vanadyls absorb in the same region (800–1000 cm^{-1}) and cannot be discriminated. Monomeric vanadyls may be evidenced after dehydration by a well resolved peak at 1020–1030 cm^{-1}. We have thus performed *in situ* spectra at room temperature of C2, C4, and C7 catalysts after calcination under dry air at 400°C. The results, however, are very similar to that of non-treated samples. In particular, the spectra do not exhibit any clear feature in the 1020–1030 cm^{-1} region, suggesting that vanadium preferentially forms polyvanadate chains in the three cases. From the frequencies region of the band, it is apparent that these species are mono-oxo vanadates (Table 4). The shift to higher frequencies and the sharpening of the Raman band with increasing coverage observed in the hydrated samples, Fig. 8, has already been observed for other supported oxides (9) and has been attributed to an increase of lateral interactions between surface species.

DISCUSSION

This section has been divided into three parts in order to discuss successively the vanadate adsorption process, the transformations occurring during the calcination and the catalytic reaction.

(*a*) *Adsorption Process*

Continuous adsorption was selected for vanadium deposition, because the method allows for the minimum contact time between the support and the vanadium solution, limiting possible by-reactions.

Three different pH's for the adsorption solution were used to control the initial vanadium environment, respectively, tetrahedral for $V_3O_9^{3-}$, $V_4O_{12}^{4-}$ (pH 7.0) and octahedral for $V_{10}O_{28}^{6-}$ (pH 4.5) and $V_{10}O_{28}H^{5-}$ (pH 2.5). The results of ^{51}V NMR and UV–visible spectroscopy related to dried samples clearly show that γ-alumina adsorbs vanadate species without change of valence state and local environment of vanadium, as (i) no V^{4+} signal is observed by UV–visible and (ii) ^{51}V NMR spectrum lines correspond to tetrahedral species for D7 and principally octahedral species for D2. Sample D4 shows a mixture of both environments. We can thus conclude that polyvanadates are adsorbed without strong local modification at ambient temperature. This observation appears surprising since we know that polymolybdates and phosphomolybdates are decomposed to MoO_4^{2-} species on contact with alumina (24), but it is not unexpected as it is known that decavanadate ions are rather difficult to revert to tetrahedral species. By analogy, and considering that the reaction in solution is pH-dependent (25), we attribute the decavanadate stability to the weak basic strength of the γ-alumina surface. It has been verified that stronger basic oxides such as MgO readily decompose the decavanadate ion in the same conditions (26).

The origin of the adsorption phenomenon is somewhat controversial. Two mechanisms are discussed in the literature. It has been previously proposed that the surface charge, determined by the relative position of the pH of the solution and the isoelectric point (IEP) of the support, is compensated by adsorption of ions of opposite charge from the solution (27). This is a purely electrostatic process. Numerous experimental evidence supports these views. However, a mechanism involving Lewis acid sites (coordinatively unsaturated surface Al^{3+}) in parallel to basic OH hydroxyls has been suggested, and experimentally checked in the case of molybdates adsorption (23). Our study in the near infrared region shows that both sites are also involved for vanadate adsorption. The strong decrease of the coordinated water band at 5310 cm^{-1} suggests that polyvanadate species are adsorbed on coordinatively unsaturated Al cations (Lewis acid sites). The adsorption mechanism should thus involve some equilibrium displacement of coordinated water as in the equation

$$Al\text{–}OH_2 + V_xO_y^{n-} \rightarrow Al\text{–}OV_xO_{y-1}^{n-} + H_2O,$$

which, in turn, is allowed by the superficial charge of the support, compensating the anion charge.

(*b*) *Calcination*

UV–visible spectroscopy shows that in all samples, vanadium retains the oxidation V^{5+} after calcination. However, the band shift towards 400 nm indicates an evolution in the vanadium environment. ^{51}V NMR spectroscopy confirms that the vanadium coordination is predominantly tetrahedral with a high connectedness after calcination. The octahedral contribution appears to be

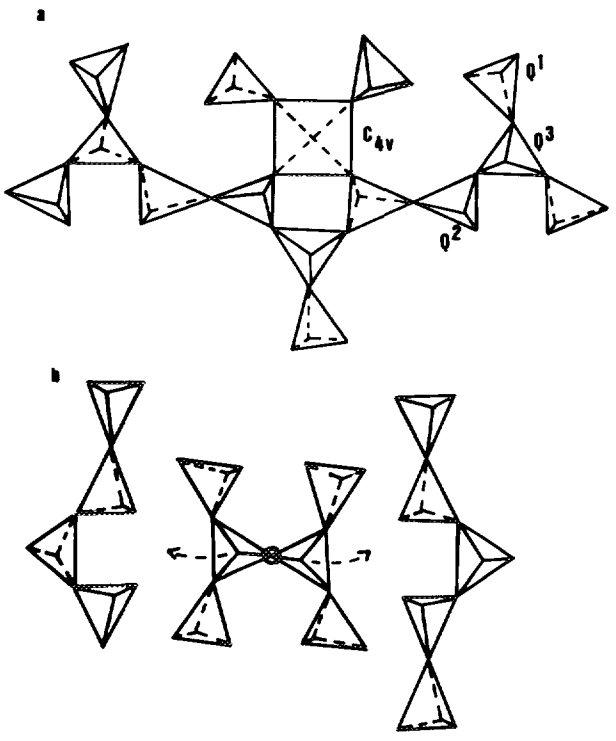

FIG. 9. (a) Structure of amorphous V_2O_5 showing linear fragments Q^2 interconnected by Q^3 and reduced V=O vanadate species. (b) Structural model for catalytic site transformation after reduction by propane. After remotion of the central (marked) bridging oxygen, the two V=O groups shift towards a $C4_v$ environment (arrows) (see text).

independent upon the solution adsorption pH or the superficial coverage.

From Raman spectra, it has been inferred that monooxo polyvanadates chains, characterized by a large band at approximately 980 cm^{-1}, are present in all samples, but show a higher degree of lateral interaction with increasing coverage, as the pH of the adsorption solution is diminished. Dioxovanadates or distorted mono-oxo VO_4 surface species are detected in minor concentration in all samples but mainly in C7 and C4 (compare the band at 945 cm^{-1}).

It is currently accepted that, on alumina support, the vanadium environment goes from tetrahedral (Q^2 species) at low coverage to octahedral at high coverage (11). Above the monolayer, crystalline vanadium pentoxide is formed. However, a tetrahedral bidimensional array has also been characterized at the monolayer value (13). At intermediate coverage, the situation is not very clear. As a matter of fact, we should expect a progressive condensation from isolated vanadate species to crystalline oxide with increasing coverage.

Two variables are therefore necessary to describe the superficial vanadate oxide layer prepared in this work: the condensation degree (Q^2 or Q^3 species) and the mean distance between neighbouring chains (lateral interactions). A model for the vanadium oxide surface is represented in Fig. 9. According to our ^{51}V NMR and Raman data, it appears that the mean separation distance between polyvanadates might decrease critically from C7 to C2 sample.

(c) *Propane Oxidative Dehydrogenation*

The V^{5+} UV–visible and ^{51}V NMR spectra do not show any significant modification in the catalyst after use, which proves that the V^{5+} structure is stable under catalytic conditions.

UV–visible and ESR spectroscopies show the presence of V^{4+} in $C4_v$ symmetry in these samples. It is interesting to note that the V^{4+} concentration follows the same ordering as catalytic activity. We note however, that catalytic activity is by no means correlated to vanadium concentration. We have shown that very active catalysts for propane ODH are obtained when γ-alumina is covered with a vanadate layer near the monolayer value. Moreover, the unique selectivity-conversion curve obtained for all catalysts has led us to postulate that a single active site is present in all samples. Since the nature of the vanadate chains appears, on the basis of ^{51}V NMR spectroscopy to be similar in the three samples, we assume that the catalytic activity of the vanadium oxide layer is determined by the mean distance between vanadate chains. We suggest that the active site in propane ODH might be the result of the cooperation of linear or branched chains. The fit of the V^{4+} ESR parameters with that observed for amorphous V_2O_5 supports the view that Q^3 species might be involved in the reaction. The high selectivity of amorphous oxides has yet been observed in other conditions (28). The model is chemically attractive: the reduction of dioxovanadates should clearly be difficult as we know the strong preference of V^{4+} ion for the monoxo vanadyl V=O structure. The high flexibility of the superficial Q^3 array should also allow the facile reduction of the mono-oxo Q^3 (four-coordinated) structure to mono oxo Q^4 (five-coordinated) reduced one.

We tentatively present, in Fig. 9, a model for the structural transformation occurring after reduction of the vanadate array. Bridging V–O–V oxide ions between two Q^3 species (see Fig. 9b) are considered here to be removed to generate two V^{4+} cations. We propose that the vanadate structure relaxes by linking the V=O group to two Q^2 vanadium cations of a neighbouring chain. The resultant structure should be comparable with that of amorphous V_2O_5 (29) (Fig. 9a). This conclusion which emphasizes the role of bridging V–O–V for propane oxydehydrogenation is in agreement with the observation of the specificity of the α-$Mg_2V_2O_7$ pyrovanadate phase for this reaction, for which the structure consists of rows of V_2O_7 groups with long V–O–V bridges (18).

ACKNOWLEDGMENTS

Catalysts were prepared at the Instituto Militar de Engenharia, Rio de Janeiro, Brazil. The experimental work was carried out at the Institut de Recherches sur la Catalyse, CNRS, France, within the France–Brazil cooperation program. We thank CNP_q, Conselho Nacional de Desenvolvimento Cientifico e Tecnologico of Brazil for financial support. We thank Dr. V. Soenen for the propane ODH measurements and Dr. F. Lefebvre for the ^{51}V NMR spectra. We acknowledge Dr. J. C. Védrine for fruitful discussion. We are grateful to the Instituto Nacional de Tecnologia of Brazil, Rio de Janeiro, for supporting one of us during the preparation of the manuscript.

REFERENCES

1. Oyama, S. T., and Somorjai, G. A., *J. Phys. Chem.* **94,** 5022 (1990).
2. Oyama, S. T., Middlebrook, A. M., and Somorjai, G. A., *J. Phys. Chem.* **94,** 5029 (1990).
3. Schraml-Marth, M., Wokaun, A., and Baiker, A., *J. Catal.* **124,** 86 (1990).
4. Centi, G., Giamello, E., Pinelli, D., and Trifiro, F., *J. Catal.* **130,** 220 (1991).
5. Centi, G., Pinelli, G., Trifiro, F., Ghoussoub, D., Guelton, M., and Gengembre, L., *J. Catal.* **130,** 238 (1991).
6. Pries de Oliveira, P. G., Lefebvre, F., Primet, M., Eon, J. G., and Volta, J. C., *J. Catal.* **130,** 293 (1991).
7. Pries de Oliveira, P. G., Eon, J. G., and Volta, J. C., *J. Catal.* **137,** 257 (1992).
8. Cristiani, C., Forzatti, P., and Busca, G., *J. Catal.* **116,** 586 (1989).
9. Went, G. T., Oyama, S. T., and Bell, A. T., *J. Phys. Chem.* **94,** 4240 (1990).
10. Chan, S. S., Wachs, I. E., Murrel, L. L., Wang, L., and Keith Hall, W., *J. Phys. Chem.* **88,** 5831 (1984).
11. Eckert, H., and Wachs, I. E., *J. Phys. Chem.* **93,** 6796 (1989).
12. Tanaka, T., Yamashita, H., Tsuchitani, R., Funabiki, T., and Yoshida, S., *J. Chem. Soc. Faraday Trans 1* **84** (9), 2987 (1988).
13. Bergeret, G., Gallezot, P., Chary, K. V. R., Rama Rao, B., and Subrahmanyam, V. S., *Appl. Catal.* **40,** 191 (1988).
14. Bond, G. C., *J. Catal.* **116,** 531 (1989).
15. Went, G. T., Leu, L. J., and Bell, A. T., *J. Catal.* **134,** 479 (1992).
16. Baes, C. F., Jr., and Mesmer, R. E., "The Hydrolysis of Cations." Wiley, New York, 1970; Deo, G., and Wachs, I. E., *J. Phys. Chem.* **95,** 5889 (1991).
17. Subramanian, S., Schwartz, J. A., and Hejase, Z., *J. Catal.* **117,** 512 (1989).
18. Siew Hew Sam, D., Soenen, V., and Volta, J. C., *J. Catal.* **123,** 417 (1990).
19. Busca, G., Marchetti, L. J., Centi, G., and Trifiro, F., *J. Chem. Soc. Faraday Trans. 1* **81,** 1003 (1985).
20. Little, L. H., Kiselev, A. V. and Lygin, V. I., "Infra-red Spectra of Adsorbed Species," Chap. 9. Academic Press, New York, 1966.
21. Ballutaud, D., Bordes, E., and Courtine, P., *Mater. Res. Bull.* **17,** 519 (1982).
22. Ballutaud, D., R'Kha, C., Gharbi, N., Michaud, M., and Livage, J., *in* "4th Conference on Reactivity of Solids, Krakow, 1980."
23. Roozeboom, F., Mittelmeijer-Hazeleger, M. C., Moulin, J. A., Medema, J., De Beer, V. H. J., and Gellings, P. J., *J. Phys. Chem.* **84,** 2783 (1980).
24. Van Veen, J. A. R., Hendricks, P. A. J. M., Romers, E. J. G. M., and Andrea, R. R., *J. Phys. Chem.* **94,** 5275 (1990).
25. Howarth, O. W., and Richards, R. E., *J. Chem. Soc. (A),* 1087 (1966).
26. Goes, E. F., and Eon, J. G., unpublished results.
27. Spanos, N. Vordonis, L., Kordulis, Ch., and Lycourghiotis, A., *J. Catal.* **124,** 301 (1990); Wang, L., and Keith Hall, W., *J. Catal.* **77,** 232 (1982); Kasztelan, S., Grimblot, J., Bonnelle, J. P., Payen, E., Toulhouat, H., and Jacquin, Y., *Appl. Catal.* **7,** 91 (1983).
28. Gasser, D., and Baiker, A., *J. Catal.* **113,** 325 (1988).
29. Mosset, A., Lecante, P., Galy, J., and Livage, J., *Philos. Mag. (8)* **46** (2), 137 (1982).
30. Wells, A. F., "Structural Inorganic Chemistry," 4th ed. Clarendon, Oxford, 1975.